# Closure of an Aortocardiac Fistula in a Horse



Lindsay J. Deacon, DVM, Cris Navas de Solis, LV, MS, PhD, DACVIM-LA, Dean W. Richardson, AB, DVM, DACVS, Amy Polkes, DVM, DACVIM, and Virginia B. Reef, BA, DVM, DACVIM, DACVSMR, *Littleton, Colorado; Kennett Square, Pennsylvania; and Darnestown, Maryland*

## INTRODUCTION

Aortic root rupture in horses is uncommon; however, awareness of the condition has heightened throughout the sport horse community in recent years due to increasing concern about horse and rider safety. It occurs most frequently at the right sinus of Valsalva, similar to the case in humans, and can result in an aortocardiac fistula (ACF).[1,2] While aortic rupture in the absence of a preexisting aneurysm is rare in humans,[2] there are multiple reports of spontaneous rupture in the horse.[1,3-5] Sudden development of an ACF can lead to life-threatening hemodynamic changes and therefore poses a safety risk to both the horse and humans involved. Classic clinical signs of aortic root rupture include development of a continuous murmur, tachycardia, exercise intolerance, signs of acute distress, and sudden death.[1,4] Echocardiography is the primary imaging modality to confirm the presence of ACF in equids. At this time, the use of multimodal imaging including transesophageal echocardiography, standard and computed tomography angiography, and cardiac magnetic resonance imaging is restricted in the horse due to patient size. Treatment options are limited and consist primarily of supportive care and management of sequelae such as ventricular arrhythmias and congestive heart failure. There are two case reports of interventions to repair ACFs in the horse[6,7]; however, this option is typically limited by visibility of the defect with available imaging modalities, its size, access, and graft/occluder device size availability.

We describe a unique case of an ACF that developed in a hospitalized equine patient, with echocardiographic evidence of closure approximately 6 weeks later. We discuss the principles of diagnosis, treatment, and long-term management of this case.

## CASE PRESENTATION

A 362 kg, 21-year-old Paso Fino gelding presented for arthrodesis of the left front proximal interphalangeal joint (PIPJ) due to end-stage osteoarthritis and persistent lameness. Seven years prior, the gelding similarly underwent arthrodesis of the right front PIPJ.

On presentation, the gelding was bright and alert, with mild left forelimb lameness observed at the walk. Vital parameters were within the normal reference ranges, and no murmurs or arrhythmias were heard on cardiac auscultation by the intaking surgical team consisting of a student, surgical resident, and anesthesiologist. Following radiographic evaluation of the left front PIPJ, the gelding was anesthetized and a left front PIPJ arthrodesis was performed using an open approach to the dorsal aspect of the joint, involving placement of two 5.5 mm transarticular screws followed by a three-hole PIPJ locking plate under fluoroscopic guidance. General anesthesia throughout the surgery was uneventful, with normal arterial blood pressures. The gelding was treated with perioperative intravenous antimicrobials (potassium penicillin, gentamicin), local antimicrobials (amikacin regional limb perfusions), anti-inflammatories (phenylbutazone), and a perioperative distal limb locoregional anesthetic block with bupivacaine.

Nineteen days postoperatively, the gelding developed a surgical site infection while in hospital. Treatment included removal of the bone plate, systemic antimicrobials (enrofloxacin), local antimicrobials (amikacin-impregnated polymethylmethacrylate beads, amikacin regional limb perfusions), anti-inflammatories (phenylbutazone), and long-acting local anesthesia (bupivacaine liposome injectable suspension).

Fifty-two days postoperatively, cardiac auscultation as part of the daily physical examination in hospital revealed a grade 4/6 continuous murmur with point of maximal intensity over the tricuspid valve area and a grade 3/6 coarse band-shaped holosystolic murmur with point of maximal intensity over the aortic and pulmonic valve areas. Initial auscultation was performed by a veterinary student and was confirmed by one fellow and two internists specializing in cardiology. Auscultation of bilateral lung fields at rest revealed normal bronchovesicular sounds. Facial arterial pulses were bounding. Noninvasive blood pressure obtained with a tail cuff and an oscillometric monitor was 133/55 (mean 86) mm Hg, and cardiac troponin I was 0.02 ng/mL (reference range, 0.00-0.07 ng/mL; $T_{1/2}$ of 0.47 hours). An echocardiogram revealed aortic root rupture with an ACF connecting the right sinus of Valsalva directly with the right ventricle, underneath the septal leaflet of the tricuspid valve (Figure 1A–C, Videos 1 and 2). There was also subendocardial dissection of blood along the left side of the interventricular septum creating a large subendocardial pouch, which communicated with the left ventricle caudally through a small endocardial tear (Figure 2A and B, Videos 3-5). The left atrium and left ventricle were mildly enlarged. Allometric scaling was used to document enlarged left atrial and left ventricular diameters, since there are no normal published values for echocardiographic measurements in Paso Finos.[8,9] The left ventricle was hyperdynamic, likely associated with increased sympathetic tone, tachycardia, and left ventricular volume overload. Color flow M-mode and color flow Doppler interrogation of the defect revealed a turbulent jet through the ACF from the aorta into the right ventricle (Figure 3A, Video 6). Continuous-wave Doppler echocardiography revealed a peak shunt

From the Littleton Equine Medical Center, Littleton, Colorado (L.J.D.); Department of Clinical Studies, University of Pennsylvania New Bolton Center, Kennett Square, Pennsylvania (C.N.d.S., D.W.R., V.B.R.); and Equine Internal Medicine and Diagnostic Services, Darnestown, Maryland (A.P.).

Keywords: Horse, Equine, Aortocardiac fistula, Subendocardial dissection, Echocardiography

Conflicts of Interest: None.

*CASE* is grateful to Boehringer Ingelheim Animal Health for their generous support to cover the processing fee for this case report.

Correspondence: Lindsay J. Deacon, DVM, Littleton Equine Medical Center, 8025 South Santa Fe Drive, Littleton, CO 80120 (E-mail: *ldeacon@littletonequine.com*).



2468-6441

https://doi.org/10.1016/j.case.2021.11.007

## VIDEO HIGHLIGHTS

**Video 1:** Echocardiogram of the ACF imaged from the right parasternal window, immediately after ACF diagnosis. The ACF is imaged between the right sinus of Valsalva and the right ventricle, extending underneath the septal leaflet of the tricuspid valve. This video was obtained in the left ventricular outflow tract view. The right ventricular inlet is displayed in the near field.

**Video 2:** Echocardiogram of the ACF imaged from the right parasternal window, immediately after ACF diagnosis. The ACF is imaged from the right sinus of Valsalva into the right ventricle in the short-axis view of the aortic valve. The aortic valve cusps and left coronary artery are labeled in Figure 1C. The right coronary artery is imaged extending cranially from the right sinus of Valsalva.

**Video 3:** Echocardiogram of the subendocardial dissection of blood on the left ventricular side of the interventricular septum, obtained from a right parasternal window immediately after ACF diagnosis. There is a large subendocardial pouch on the left side of the interventricular septum imaged from the standard four-chamber view. The right ventricular inlet is displayed in the near field.

**Video 4:** Echocardiogram of the subendocardial dissection of blood on the left ventricular side of the interventricular septum, obtained from a right parasternal window immediately after ACF diagnosis. There is a large subendocardial pouch on the left side of the interventricular septum imaged from the short-axis view of the left ventricle.

**Video 5:** Echocardiogram of the subendocardial dissection of blood on the left ventricular side of the interventricular septum and the small rupture into the left ventricle, obtained from a right parasternal window immediately after ACF diagnosis. This color flow Doppler echocardiogram demonstrates the small rupture from the subendocardial dissection into the left ventricle. The right ventricular inlet is displayed in the near field.

**Video 6:** Color flow Doppler echocardiogram of the ACF imaged from the right parasternal window immediately after ACF diagnosis. The ACF is imaged between the right sinus of Valsalva and the right ventricle, extending underneath the septal leaflet of the tricuspid valve containing a narrow high-velocity turbulent jet going from left to right. This video was obtained in the left ventricular outflow tract view, with the right ventricular inlet displayed in the near field.

**Video 7:** Color flow Doppler echocardiogram of the narrow low-velocity shunt into the left ventricle, imaged in the short-axis view of the left ventricle just underneath the mitral valve. This video was obtained from a right parasternal window immediately after ACF diagnosis.

**Video 8:** Four-dimensional echocardiogram of the ACF associated with the aortic root rupture at the right sinus of Valsalva. Color flow Doppler reveals the ACF shunt between the right sinus of Valsalva and the right ventricle. This video was obtained from a right parasternal window immediately after ACF diagnosis.

**Video 9:** Four-dimensional echocardiogram of the subendocardial dissection and subendocardial pouch on the left side of the interventricular septum associated with the aortic root rupture at the right sinus of Valsalva. This video was obtained from a right parasternal window immediately after ACF diagnosis.

**Video 10:** Two-dimensional echocardiogram of the area of the prior ACF where the fistula is no longer visible. The endocardium and subendocardium where it was previously detected now appears hyperechoic and thickened. This video sweeps cranial to caudal through the left ventricular outflow tract. The right ventricular inlet is displayed in the near view. This video was obtained from a right parasternal window 634 days after discharge from the hospital. It is reflective of the echocardiogram performed 2 weeks after discharge, as the appearance of the prior ACF remained unchanged.

**Video 11:** Two-dimensional echocardiogram of the area of the prior ACF where the fistula and subendocardial pouch are no longer visible. The endocardium and subendocardium where they were previously detected now appear hyperechoic and thickened. This video sweeps dorsal to ventral through the aorta, mitral valve, and left ventricle at the chordal level. The right ventricle is displayed in the near view. This video was obtained from a right parasternal window 634 days after discharge from the hospital. It is reflective of the echocardiogram performed 2 weeks after discharge, as the appearance of the prior ACF remained unchanged.

**Video 12:** Color flow Doppler echocardiogram sweeping cranial to caudal through the left ventricular outflow tract. The right ventricular inlet is displayed in the near view. The previously detected left-to-right shunt from the right coronary sinus into the right ventricle is no longer observed. This video was obtained from a right parasternal window 634 days after discharge from the hospital. It is reflective of the echocardiogram performed 2 weeks after discharge, as the appearance of the prior ACF remained unchanged.

**Video 13:** Color flow Doppler echocardiogram of the short-axis aorta. The right atrium and ventricle are displayed in the near view. The previously detected left-to-right shunt from the right coronary sinus into the right ventricle is no longer observed, nor is the previously detected shunt from the subendocardial pouch into the left ventricle. This video was obtained from a right parasternal window 634 days after discharge from the hospital. It is reflective of the echocardiogram performed 2 weeks after discharge, as the appearance of the prior ACF remained unchanged.

**View the video content online at www.cvcasejournal.com.**

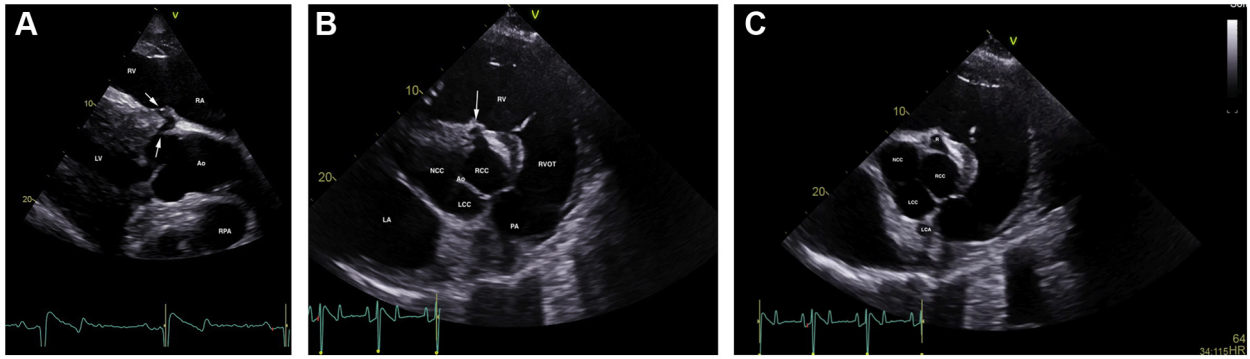


**Figure 1** Two-dimensional echocardiograms performed immediately after ACF diagnosis, illustrating the ACF (*white arrows*) extending from the right sinus of Valsalva to the right ventricle, underneath the septal leaflet of the tricuspid valve. **(A)** Long-axis view of the left ventricular outflow tract obtained from the right parasternal window. The right ventricular inlet is displayed in the near field. **(B)** Short-axis view of the aorta obtained from the right parasternal window, highlighting the ACF (*white arrow*). **(C)** Short-axis view of the aorta obtained from the right parasternal window, illustrating the site of the rupture (R) and LCA. The right coronary artery is not imaged in this figure but is visible in Video 1. *Ao*, Aorta; *LA*, left atrium; *LCA*, left coronary artery; *LCC*, left coronary cusp; *LV*, left ventricle; *NCC*, noncoronary cusp; *PA*, pulmonary artery; *RA*, right atrium; *RCC*, right coronary cusp; *RPA*, right pulmonary artery (cross-section); *RV*, right ventricle; *RVOT*, right ventricular outflow tract.

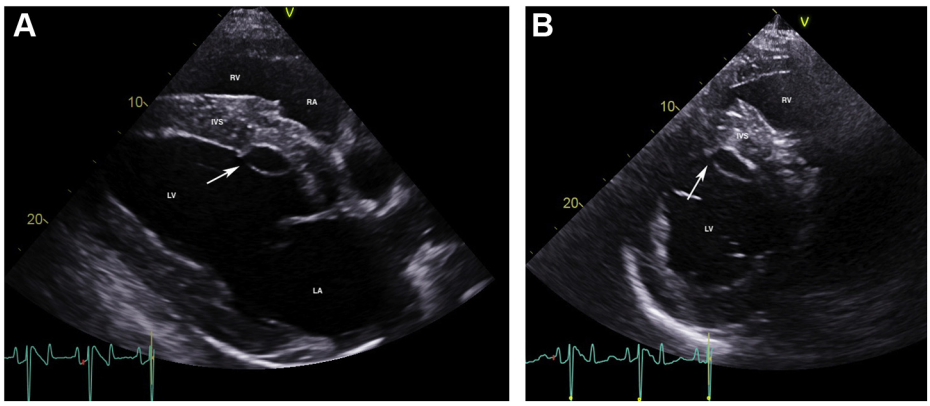


**Figure 2** Two-dimensional echocardiograms performed immediately after ACF diagnosis, illustrating subendocardial dissection of blood along the left side of the interventricular septum, resulting in a large anechoic subendocardial pouch. The site of endocardial rupture is indicated (*arrow*). **(A)** Long-axis four-chamber view of the heart obtained from the right parasternal window. The right ventricular inlet is displayed in the near field. **(B)** Short-axis view of the left ventricle at the chordal level obtained from the right parasternal window. *IVS*, Interventricular septum; *LA*, left atrium; *LV*, left ventricle; *RA*, right atrium; *RV*, right ventricle.

velocity of 4.2 m/sec in systole and 5.2 m/sec in early diastole, with a rapid decline in maximal velocity (Figure 3B). Turbulent blood flow was also detected in the subendocardial defect, with a small area located caudally where blood was entering the left ventricle through an endocardial tear (Figure 4A and B, Videos 5 and 7). There were no significant valvular regurgitant jets. Four-dimensional echocardiography provided real-time insight into the three-dimensional conformation of the ACF in relation to its surrounding structures (Figure 5A and B, Videos 8 and 9). The wide pulse pressure is likely due to the diastolic runoff into the right (primarily) and left ventricles.

Continuous telemetric electrocardiographic monitoring of the gelding's cardiac rhythm for 5 days revealed normal sinus rhythm with no significant ventricular ectopy. The gelding was started on benazepril at a dose of 1.0 mg/kg every 12 hours after the ACF was diagnosed. He remained in the hospital for an additional month for continued orthopedic treatment and cardiac monitoring. Upon discharge 32 days after initial diagnosis of the ACF, the cardiac murmur remained unchanged.

A cast change was performed 2 weeks after discharge, at which time the murmur was no longer evident. This examination was performed by a boarded internist with cardiac auscultation skill equivalent to the specialists in hospital. Cardiac evaluation revealed a normal heart rate, hyperkinetic peripheral arterial pulses, and a grade 2/6 diastolic murmur with point of maximal intensity over the aortic valve, with no auscultable murmur on the right. An echocardiogram revealed mild aortic regurgitation and no change in cardiac dimensions compared with the initial exam. The ACF and subendocardial pouch were no longer visible. The endocardium and subendocardium

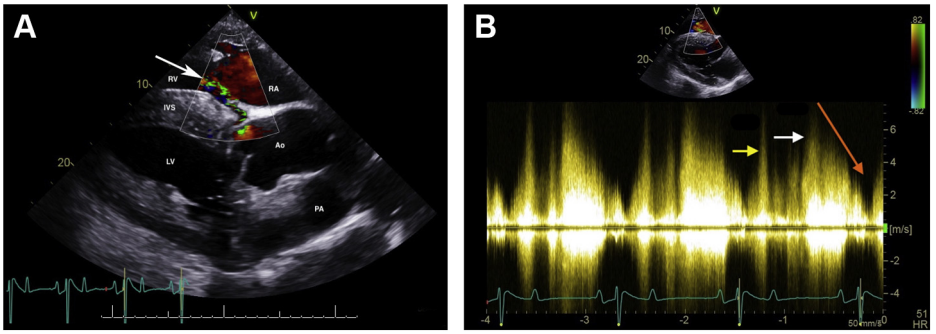


**Figure 3** Color flow Doppler **(A)** and continuous-wave Doppler echocardiography **(B)** of the left-to-right shunt through the ACF from the right sinus of Valsalva into the right ventricle. All images were obtained from the right parasternal window immediately after ACF diagnosis. **(A)** Color Doppler two-dimensional echocardiogram of the left-to-right shunt through the ACF from the right sinus of Valsalva into the right ventricle, underneath the septal leaflet of the tricuspid valve (*arrow*), in the left ventricular outflow tract view. The right ventricular inlet is displayed in the near field. **(B)** Continuous-wave Doppler echocardiography demonstrating a peak shunt velocity of 4.2 m/sec in systole (*yellow arrow*) and 5.2 m/sec in early diastole (*white arrow*), with a rapid decline in maximal velocity (steep diastolic runoff; *orange arrow*). *Ao*, Aorta; *IVS*, interventricular septum; *LV*, left ventricle; *PA*, pulmonary artery; *RA*, right atrium; *RV*, right ventricle.

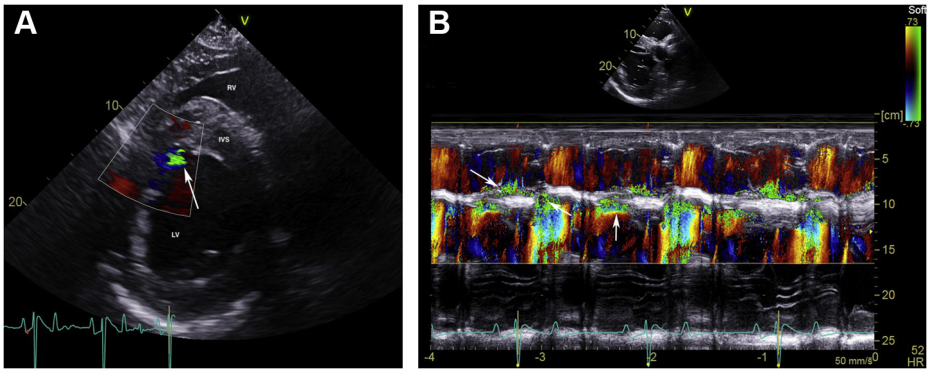


**Figure 4** Color flow Doppler **(A)** and color M-mode echocardiography **(B)** of the left-to-right shunt through the ACF with subendocardial dissection and a small jet extending into the left ventricle (*arrow*). All images were obtained from the right parasternal window immediately after ACF diagnosis. **(A)** Color Doppler two-dimensional echocardiogram of the shunt into the left ventricle along the caudal edge of the subendocardial dissection (*arrow*) in the short-axis view of the left ventricle, just below the mitral valve. **(B)** Color M-mode echocardiogram of the left-to right shunt through the ACF and turbulent flow in the subendocardial dissection obtained from the short-axis view between the aorta and mitral valve. The *vertical arrow* demonstrates turbulence in the subendocardial dissection, while the *diagonal arrows* represent turbulence from the right sinus of Valsalva into the right ventricle. *IVS*, interventricular septum; *LV*, left ventricle; *RV*, right ventricle.

at the site of the subendocardial dissection were hyperechoic and thickened, as was the area along the right sinus of Valsalva where it previously communicated with the right ventricle. Recheck auscultation and echocardiograms were performed 6, 29, and 90 weeks later by boarded internists and specialists in cardiology and revealed no changes compared with the examination 2 weeks post discharge. Cardiac reevaluation on day 634 confirmed the aforementioned findings (Figure 6, Videos 10 and 11). Color flow Doppler echocardiography revealed no flow at the site of the previous ACF or the subendocardial dissection at the time of both examinations (Videos 12 and 13). Simultaneous electrocardiograms on all recheck exams revealed normal sinus rhythm.

The gelding was continued on benazepril, even though the aortic regurgitation was only mild, to reduce systemic arterial blood pressure. It was recommended that the gelding not be ridden due to the risk of sudden reopening of the ACF with elevation of systemic pressures during exercise and a subsequent catastrophic cardiac event. Annual recheck echocardiography was recommended, along with routine auscultation for the recurrence of a continuous murmur.

## DISCUSSION

Aortic root rupture was first reported in breeding stallions in 1967.[3] It has since been observed in a variety of breeds, including the Standardbred, Thoroughbred, Thoroughbred cross, quarter horse cross, Paso Fino, Arabian, and American saddlebred. The aortic root rupture usually occurs at the right sinus of Valsalva, resulting in an ACF.[1,3,5,10,11] Aortocardiac fistula can occur secondary to rupture of a sinus of Valsalva aneurysm or rupture of the aortic root, without a preexisting aneurysm.[1,4] In nearly all ACF cases, the rupture occurs

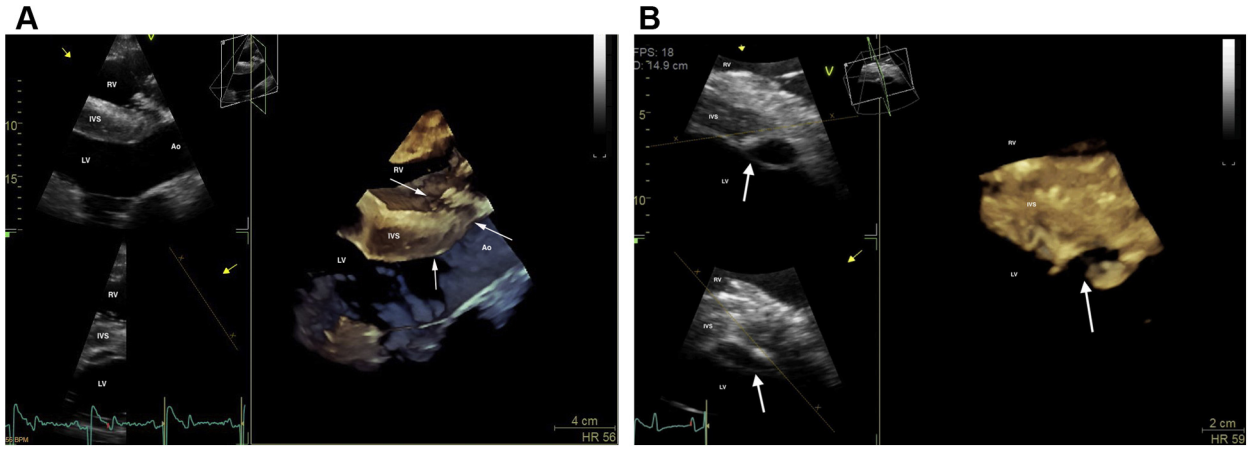


**Figure 5** Three-dimensional (3D) echocardiograms of the ACF **(A)** and the subendocardial dissection **(B)** obtained from the right parasternal window immediately after ACF diagnosis. **(A)** Modified long-axis 3D image of the left ventricular outflow tract with slight cranial and dorsal obliquity. The right ventricular inlet is displayed in the near field. *Arrows* are pointing to the ACF. **(B)** Short-axis 3D image of the left ventricle, just below the mitral valve. The right ventricle is displayed in the near field. Arrows are pointing to the subendocardial dissection. *Ao*, Aorta; *IVS*, interventricular septum. *LV*, left ventricle; *RV*, right ventricle.

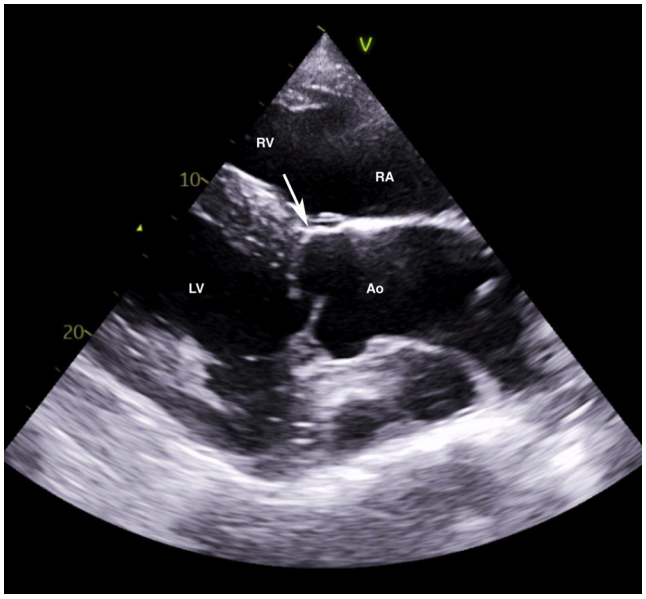


**Figure 6** Two-dimensional echocardiogram of the left ventricular outflow tract view obtained from a right parasternal window, similar to Figure 1, performed 2 weeks after discharge from the hospital with identical findings on day 634 post discharge. The right ventricular inlet is displayed in the near field. Notice that the previously detected ACF (*arrow*) is no longer visible. *Ao*, Aorta; *LV*, left ventricle; *RA*, right atrium; *RV*, right ventricle.

in the right sinus of Valsalva, extending into the right atrium or right ventricle or, less frequently, through the tricuspid valve or into the left ventricle. Most horses are middle aged when the ACF develops, even if they rupture a preexisting aneurysm. Male horses predominate in the literature, similar to the situation in human beings. There has only been one horse with a congenital defect (ventricular septal defect) reported with ACF secondary to rupture of a sinus of Valsalva aneurysm.[4] In contrast, Friesians typically develop aortopulmonary fistulation characterized by aortic rupture at the ligamentum arteriosum.[12]

The classically described clinical signs of ACF include development of a continuous machinery murmur, signs of acute pain and distress that are often mistaken for colic, or sudden death. Ventricular tachycardia has been detected in some horses that present acutely, usually resolving with time or antiarrhythmic therapy. On rare instances, ACF has been reported as an incidental finding.[1] This case highlights the varied clinical signs at presentation, as a continuous murmur was the sole clinical sign seen in our patient. However, it is possible that the gelding demonstrated transient signs of distress overnight that were not directly observed. We hypothesize that the rupture was due to chronic weakening of the aortic root, possibly associated with a connective tissue disorder and systemic hypertension associated with chronic pain.

Differential diagnoses for a continuous murmur in this patient include a ventricular septal defect with secondary aortic regurgitation due to aortic valve prolapse, aortic valve endocarditis with spread into the adjacent tissue of the interventricular septum (with or without subsequent ACF formation), patent ductus arteriosus, or coronary-to-cardiac fistula. Ventricular septal defect and patent ductus arteriosus were ruled out based on echocardiographic examination, with the latter being very rare in horses. Aortic valve endocarditis was a consideration given the patient's history of surgical site infection; however, echocardiographic evidence of endocarditis could not be demonstrated. To our knowledge, coronary-to-cardiac fistulation has never been reported in horses, and this patient had two normal coronary arteries (Figure 1C, Video 2).

Aortocardiac fistulation has been reported in many breeds, with the Paso Fino anecdotally overrepresented in the population of affected horses. The Paso Fino and Peruvian Paso are also more commonly affected by degenerative suspensory ligament desmitis (DSLD) compared with other breeds.[13] This disease is characterized by abnormal proteoglycan deposition within connective tissues and abnormal collagen within ligaments. Histologic examination of other body systems in horses affected by DSLD revealed abnormal collagen fibrils within the media of the aorta, which has the potential to

contribute to aortic weakening and subsequent rupture. However, further research is required to investigate whether connective tissues diseases or horses with DSLD have a higher incidence of ACF compared with the general population and to confirm that these breeds (Paso Fino and Peruvian Paso) are disproportionately represented.

Our patient had a history of chronic pain secondary to severe degenerative joint disease, which may have resulted in periodic increases in systemic arterial blood pressure and weakening of the aortic wall. There is a single report of a horse with chronic renal disease, an enlarged aortic root, moderate aortic regurgitation, and systemic hypertension that developed acute distress following turnout exercise and was found to have developed an ACF.[14] This horse had severe systemic hypertension (240 mm Hg/137 mm Hg; mean arterial pressure 164 mm Hg). The resting hypertension likely increased in severity with exercise. Recent exercise is a common history in horses that develop an ACF.[1,3,11] The severe exercising hypertension, combined with aortic root enlargement and possible iatrogenic volume overload, may have led to aortic root rupture in this horse. Multiple factors, including previous hypertension associated with musculoskeletal pain and genetic factors, probably contributed to the development of the ACF in our patient.

While our patient did not have a history of recent exercise, he may have experienced other stressors in hospital that had a similar effect, raising his arterial blood pressure. Blood pressure is not routinely measured in equine surgical patients, except under general anesthesia. Horses with ACF may survive the acute event if subsequent fatal arrhythmias do not occur. However, long-term survival depends on the severity of secondary cardiac changes and associated arrhythmias and hemodynamic effects that develop.[1] The reported survival time of horses with ACF ranges from days to several years, with the latter reported in a single case.[1] The majority of horses develop congestive heart failure within days to months after the onset of clinical signs of ACF, with most developing congestive heart failure within 1 year.[1,3,4,10] While two cases of surgical intervention to occlude the ACF are reported in the horse, in both cases horses did not survive long term, and the long-term prognosis for horses with ACF remains poor.[6,7]

This case report describes spontaneous closure of an ACF in a horse that was suspected due to fibrous connective tissue filling the defects. We hypothesize that the combination of pain management, decreased stress after discharge from the hospital, and use of an angiotensin-converting enzyme inhibitor (benazepril) resulted in stabilization of systemic arterial pressures and subsequent lower pressure differentials between the aorta and cardiac chambers involved in shunting. Spontaneous closure of aortic fistulation in humans has been reported; however, the large majority of cases receive surgical intervention before spontaneous closure is possible.[15] Aortic valve prolapse into the defect could also contribute to the ACF closure, given the high-pressure difference between the aorta and right ventricle and the relatively short time for follow-up after discharge. The audible aortic regurgitation during the follow-up period supports this hypothesis; however, simultaneous closure of the small shunt into the left ventricle is less likely from the aortic valve prolapse.

We hypothesize that the gelding will have a normal lifespan, so long as the horse is not rigorously exercised, the fistula does not recur, and the aortic regurgitation does not progress. Further monitoring of horses with ACF is needed to better understand long-term outcomes; however, this unique case documents that spontaneous closure of ACF can occur in the horse.

## SUPPLEMENTARY DATA

Supplementary data to this article can be found online at https://doi.org/10.1016/j.case.2021.11.007.

## REFERENCES

1. Marr CM, Reef VB, Brazil TJ, Thomas WP, Knottenbelt DC, Kelly DF, et al. Aorto-cardiac fistulas in seven horses. Vet Radiol Ultrasound 1998;39:22-31.
2. Fennich H, Doghmi N, Rim F, Belhaj S, Cheikhi F, Cherti M. Spontaneous rupture of right aortic sinus of Valsalva leading to massive cystic dissection of interventricular septum and complete heart block. Echocardiography 2018;35:2109-12.
3. Rooney JR, Prickett ME, Crowe MW. Aortic ring rupture in stallions. Pathol Vet 1967;4:268-74.
4. Sleeper MM, Durando MM, Miller M, Habecker PL, Reef VB. Aortic root disease in four horses. J Am Vet Med Assoc 2001;15:491-6.
5. Roby KA, Reef VB, Shaw DP, Sweeney CR. Rupture of an aortic sinus in a 15-year-old broodmare. J Am Vet Med Assoc 1986;189:305-8.
6. Javsicas LH, Giguere S, Maisenbacher HW, Schmidt M, Frederick JD, Conway JA, et al. Percutaneous transcatheter closure of an aorto-cardiac fistula in a Thoroughbred stallion using an Amplatzer occluder device. J Vet Intern Med 2010;24:994-8.
7. Vernemmen I, De Clercq D, Decloedt A, Schauvliege D, Taeymans Y, De Wolf D, et al. Percutaneous transcatheter closure of an aorto-cardiac fistula in a six-year-old Warmblood mare with atrial fibrillation. J Vet Cardiol 2019;24:78-84.
8. Huesler IM, Mitchell KJ, Schwarzwald CC. Echocardiographic assessment of left atrial size and function in Warmblood horses: reference intervals, allometric scaling, and agreement of different echocardiographic variables. J Vet Intern Med 2016;30:1241-52.
9. Berthoud D, Schwarzwald CC. Echocardiographic assessment of left ventricular size and systolic function in Warmblood horses using linear measurements, area-based indices, and volume estimates: a retrospective database analysis. J Vet Intern Med 2020;35:504-20.
10. Reef VB, Klump S, Maxson AD, Sweeney RW. Echocardiographic detection of an intact aneurysm in a horse. J Am Vet Med Assoc 1990;197:752-5.
11. Lester GD, Lombard CW, Ackerman NA. Echocardiographic detection of a dissecting aortic root aneurysm in a Thoroughbred stallion. Vet Radiol Ultrasound 1992;33:202-5.
12. Ploeg M, Saey V, de Bruijn CM, Grone A, Chiers K, van Loon G, et al. Aortic rupture and aorto-pulmonary fistulation in the Friesian horse: characterization of the clinical and gross *post mortem* findings in 24 cases. Equine Vet J 2013;45:101-6.
13. Mero JL, Pool RR. Twenty cases of degenerative suspensory ligament desmitis in Peruvian Paso horses. AAEP Proc 2002;48.
14. Baker RE, Schlipf JW Jr, Scollan KF, LeBlanc NL, Russell DS. In-hospital development of an aorto-cardiac fistula in a Warmblood gelding with chronic renal disease. Equine Vet Educ 2019;33:185-7.
15. Jainandunsing JS, Linnemann R, Bouma W, Natour N, Bidar E, Lorusso R, et al. Aorto-atrial fistula formation and closure: a systematic review. J Thorac Dis 2019;11:1031-46.